Electrochemistry Communications 104 (2019) 106482

Contents lists available at ScienceDirect

Electrochemistry Communications

journal homepage: www.elsevier.com/locate/elecom

Understanding the enhanced rates of hydrogen evolution on dissolving magnesium

J.A. Yuwono[a,b,*], C.D. Taylor[c,d], G.S. Frankel[c], N. Birbilis[b,e,1], S. Fajardo[f,**,1]

[a] School of Photovoltaics and Renewable Engineering, University of New South Wales Sydney, Kensington, New South Wales 2052, Australia
[b] Department of Materials Science and Engineering, Monash University, Victoria 3800, Australia
[c] Fontana Corrosion Center, Department of Materials Science and Engineering, The Ohio State University, Columbus, OH 43210, USA
[d] Materials Technology and Development, DNV GL, Dublin, OH 43017, USA
[e] College of Engineering and Computer Science, Australian National University, Acton, Australian Capital Territory 2601, Australia
[f] Department of Surface Engineering, Corrosion and Durability, National Centre for Metallurgical Research (CENIM-CSIC), Madrid 28040, Spain

ARTICLE INFO

Keywords:
Magnesium
Hydrogen evolution
Dissolution
Density functional theory DFT
Negative difference effect NDE

ABSTRACT

Despite the growing interest in Mg and its alloys, their use has been largely limited due to their high reactivity in aqueous environments. Improving the understanding of the basic principles of Mg corrosion represents the first step to explain and, eventually, improve the corrosion behaviour of Mg alloys. Herein an original mechanistic surface kinetic DFT model that clarifies the mechanism of anomalous HE on anodically polarised Mg is presented. In accordance with several experimental observations, this model describes anomalous HE proceeding at the regions dominated by anodic dissolution via the reaction of an Mg*H intermediate with water. The Mg*H intermediates undergo oxidation upon anodic polarisation, resulting in hydrogen evolution and Mg dissolution. Furthermore, it is revealed that increasing rates of an electrochemical cathodic reaction are possible within a dissolving anode.

1. Introduction

When magnesium (Mg) is exposed to water, corrosion occurs with hydrogen evolution (from the reduction of water) as the primary cathodic reaction. According to the theory of electrochemical kinetics typified by the Butler–Volmer equation, the rate of a cathodic reaction decreases exponentially with increasing potential [1]. However, in aqueous environments, Mg exhibits the opposite behaviour with the rate of the hydrogen evolution reaction (HER) increasing with increasing anodic polarisation above the open circuit potential [2], which contradicts expectations of standard electrochemical kinetics. This behaviour, which we refer to as anomalous HE has been observed for a long time [3], but its reaction mechanism is unknown and remains a topic of intense investigation. Recent observations have determined that the vast majority of anomalous HE originates at the actively dissolving regions [4–8]. We present herein an original mechanistic surface kinetic DFT model that clarifies the mechanism of anomalous HE on anodically polarised Mg. Furthermore, it is revealed that increasing rates of an electrochemical cathodic reaction are possible within a dissolving anode.

Present theories to explain anomalous HE on anodically polarised pure Mg exposed to water include: the effect of the corrosion products, which have been shown to be more catalytic than the native metal surface towards the HER [9–14]; enrichment of metal impurities (present even in ultra-high purity Mg) during Mg dissolution, which may act as preferred sites for HE even at potentials when Mg is undergoing anodic polarisation [4,15–19]; and an impurity-based mechanism in which metal impurities present in the Mg electrode undergo non-faradaic release from dissolution of the surrounding Mg matrix and redeposit onto the electrode surface after aqueous free corrosion [7,20–23]. Even though the aforementioned phenomena are able to rationalise a source for anomalous HE, their contribution has been shown, from a range of empirical tests, to only account for a fraction of the total anomalous HE rates measured during anodic polarisation [4–7]. An accumulation of experimental evidence reveals that actively dissolving anodic regions are the primary source for anomalous HE on

* Correspondence to: J.A. Yuwono, School of Photovoltaics and Renewable Engineering, University of New South Wales Sydney, Kensington, New South Wales 2052, Australia.
** Corresponding author.
E-mail addresses: j.yuwono@unsw.edu.au (J.A. Yuwono), fajardo@cenim.csic.es (S. Fajardo).
[1] ISE member.

https://doi.org/10.1016/j.elecom.2019.106482
Received 24 May 2019; Received in revised form 11 June 2019; Accepted 17 June 2019
Available online 19 June 2019

anodically polarised pure Mg [4–6,8]. However, the mechanistic and molecular level origins of anomalous HE have not been elucidated to date.

First-principles density functional theory (DFT) calculations enable the estimation of the electrochemical activity of Mg species on surfaces and in aqueous electrolytes, providing one approach to understanding surface evolution during electrochemical/chemical reactions at the Mg/H_2O interface [24–27]. Herein we present an original mechanistic surface kinetic DFT model that clarifies the mechanism of anomalous HE on anodically polarised Mg based on prior experimental observations and supported by ab initio molecular dynamics (AIMD) simulations. Furthermore, it is revealed that increasing rates of an electrochemical cathodic reaction are possible within a net dissolving anode. This model explains the origins of the increasing rate of the cathodic HE reaction at anodic potentials, whereas previous ab initio models could not, without considering the hydroxide desorption reaction. Briefly, Taylor proposed that HE under anodic polarisation is not the result of an electrochemical reaction but the product of the chemical recombination of adsorbed hydrogen atoms on the Mg surface (i.e. Tafel pathway) [27]. However, Yuwono et al. [25] showed that the contribution of the Tafel mechanism is insignificant both under anodic and cathodic polarisation. Furthermore, the model by Yuwono et al. did not explicitly describe the regions of HE and Mg dissolution, whereas previous experimental evidence indicated that both reactions occur at the same surface regions [4–6]. Lastly, this model only accounts for anomalous HE within a very narrow window of anodic potentials and therefore cannot fully explain the numerous empirical observations of anomalous HE over large anodic overpotentials. AIMD simulations (as shown in Fig. 1, but explained below) support a model where oxidation (Mg dissolution) and reduction (HE) reactions on the Mg surface may occur simultaneously at the local active sites, not separately at distant local anodes and cathodes.

2. Computational methods

2.1. Reaction kinetic model

All reactions considered in the kinetic model are briefly introduced here and their mechanism will be discussed further in the next section. The latest experimental observations revealed that the increasing catalytic activity of Mg towards the hydrogen evolution reaction is associated with the regions undergoing active Mg dissolution [4–6,28]. This leads to the development of one possible microkinetic pathway, involving the dissolution of Mg*H from the surface (Eq. (1)). Mg*H acts as an intermediate species that assists the simultaneous Mg dissolution and HE reactions. Mg* is an available metallic Mg site on the surface. For all reactions presented below, "r_i" are the rates of reaction, "k_i" are the rate constants, and θ_H, θ_{OH} and θ_M are the surface fractional coverage of Mg*H, Mg*OH and Mg*, respectively.

$$Mg + Mg^*H + H^+ \rightarrow Mg^* + Mg^{2+} + H_2 + e^- \qquad r_1 = k_1\theta_H \tag{1}$$

The basic HE reaction pathway remains important, especially under cathodic polarisation. The Heyrovsky pathway (Eq. (2)) is used in this model considering that it occurs at a significantly higher rate than the Tafel pathway. It is important to note that the total HE rate is obtained from the combination of reactions producing H_2, Eqs. (1) and (2). The removal of Mg*H produces active sites that make the surface capable of supporting other reactions.

$$Mg^*H + H^+ + e^- \rightarrow Mg^* + H_2 \qquad r_2 = k_2\theta_H \tag{2}$$

Eqs. (3) and (4) describe the dissociation of water molecules on the Mg surface, which are followed by the adsorption of hydrogen and hydroxide ions (viz. $2Mg^* + H_2O \rightarrow Mg^*H + Mg^*OH$). Herein, the water dissociation occurs via heterolytic pathway, meaning that the rates of hydrogen and hydroxide adsorption depend on the pH and applied potential and do not equally compete in any condition, such as has been described previously in many studies [25,27].

$$Mg^* + H^+ + e^- \rightarrow Mg^*H \qquad r_3 = k_3\theta_M \tag{3}$$

$$Mg^* + OH^- \rightarrow Mg^*OH + e^- \qquad r_4 = k_4\theta_M \tag{4}$$

Water molecules assist the dissolution of Mg from the surface (viz. $Mg^* + Mg + 6\,H_2O \rightarrow [Mg(H_2O)_6]^{2+} + Mg^* + 2e^-$). Since the kinetic model herein was based on steady state equations and equilibrium coverage, Eqs. (5) and (6) include the adsorption of hydrogen and hydroxide ions to model the Mg dissolution via water-assisted reaction and to consider the changes on the surface coverage.

$$Mg^* + H^+ + Mg \rightarrow Mg^*H + Mg^{2+} + e^- \qquad r_5 = k_5\theta_M \tag{5}$$

$$Mg^* + OH^- + Mg \rightarrow Mg^*OH + Mg^{2+} + 3e^- \qquad r_6 = k_6\theta_M \tag{6}$$

Eqs. (3)–(6) exhibit the overall reduction-oxidation occurring on the

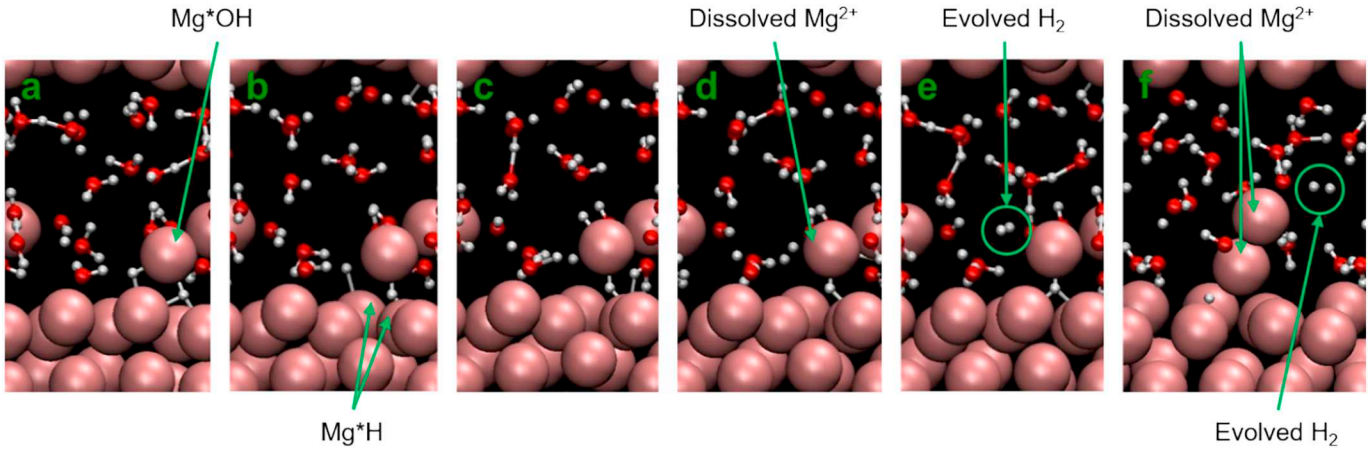

Fig. 1. Series of snapshots showing Heyrovsky HE and Mg dissolution reactions occur at the Mg/H_2O interface. The complete process of Mg interfacial reactions in water during AIMD simulation is available on the Supporting Information. Orange, red and white balls represent Mg, O and H atoms. (For interpretation of the references to colour in this figure legend, the reader is referred to the web version of this article.)

Table 1
Rate constants from ab initio simulations for the construction of Mg electrochemical kinetic model.

Reaction no.	Prefactor, k°	Energy barrier, E_a (eV)	Standard electrode potential, E° (V vs. SHE)	Dependent variable
(1)	1.0×10^{13}	1.51	−2.363	$[Mg^{2+}]$, pH
(2)	1.0×10^{13}	1.08	0	pH
(3)	1.0×10^{13}	1.06	0	pH
(4)	1.0×10^{13}	1.06	−1.862	pH
(5)	1.0×10^{13}	1.51	−2.363	$[Mg^{2+}]$, pH
(6)	1.0×10^{13}	1.51	−2.363	$[Mg^{2+}]$, pH
(8)	1.0×10^{13}	1.51	−2.363	$[MgOH^{+}]$

Notes: $[Mg^{2+}] = 2 \times 10^{-5}$ M and pH = 3, 7, 11.

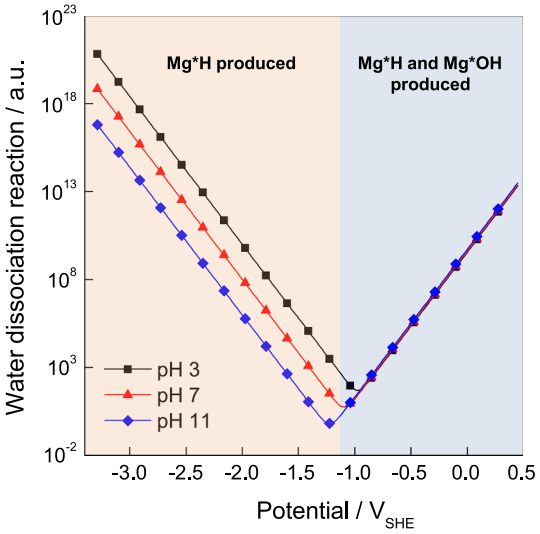

Fig. 2. Kinetic profile at different pH values of the water dissociation reaction on the Mg(0001) surface plotted as a function of potential.

Mg surface (Eq. (7)), where Mg is oxidised into Mg^{2+} and Mg*OH and water is reduced on the surface into Mg*H. In this reaction, active sites on the surface are consumed following the adsorption of hydrogen and hydroxide ions.

$$2Mg + 4\,Mg^{*} + 2H_2O \rightarrow 2\,Mg^{*}H + 2\,Mg^{*}OH + 2\,Mg^{2+} + 4e^{-} \quad (7)$$

Magnesium dissolution via OH-assisted reaction is also present along with the previous Mg dissolution via H-assisted reaction (Eq. (1)) and water-assisted (Eqs. (5) and (6)) reactions. The active sites are produced following the dissolution of Mg*OH (Eq. (8)) from the surface.

$$Mg + Mg^{*}OH \rightarrow Mg^{*} + Mg(OH)^{+} + e^{-}$$
$$r_8 = k_8\theta_{OH} \quad (8)$$

Following the reaction kinetic pathway described above, polarisation curves were developed using the formalism used on the previous studies, steady state equation and equilibrium coverage. The reaction kinetic equations are described by Eqs. (9)–(12), and their parameters for each individual reaction are presented in Table 1.

$$d\theta_M/dt = (k_1 + k_2)\theta_H + k_8\theta_{OH} - (k_3 + k_4 + k_5 + k_6)\theta_M \quad (9)$$

$$d\theta_H/dt = (k_3 + k_5)\theta_M - (k_1 + k_2)\theta_H \quad (10)$$

$$d\theta_{OH}/dt = (k_4 + k_6)\theta_M - k_8\theta_{OH} \quad (11)$$

$$\theta_M + \theta_H + \theta_{OH} = 1 \quad (12)$$

2.2. AIMD simulation

Ab initio molecular dynamics simulations were performed to analyse the interaction of water molecules with a stepped clean surface of Mg. The (311) surface was modelled, as it contains step sites that could reasonably be expected to be more reactive towards activation of water molecules, leading to hydrogen evolution, as well as potential anodic reactions such as Mg dissolution or $Mg^{*}OH_x$ formation. Since AIMD simulations have a limited access to time-scales (10–100 ps at most), the system of a stepped surface described above with a minimal slab size (3 layers), low precision, only a gamma-point mesh, and a time-step of 1.0 fs was developed so that the simulation is as time-efficient as possible with regards to accessing potential reaction chemistry. The temperature was set constant at 300 K using velocity scaling algorithm (SMASS = −1). While these settings considerably reduce the accuracy of the simulation, it is emphasised that the purpose of these AIMD simulations was to explore potentially significant surface reactivity rather than to obtain detailed kinetic or thermodynamic parameters. A total of 10.0 ps was simulated using AIMD.

Several phenomena were observed during the AIMD simulations of water on pure Mg. This condition represents the early stages of Mg free corrosion in aqueous electrolytes. Water molecules were determined to react quickly to produce Mg*OH and Mg*H on the clean Mg surface, particularly in the region of step atoms. Additionally, Mg*H on the surface interacts with water molecules near the clean Mg surface to form molecular H_2, which is emitted into the solution phase of the slab model. Finally, one of the outermost Mg atoms on the step begins to dissolve from the slab, as it interacts more with water molecules, thus showing tendency towards Mg dissolution at the same time as H_2 is being evolved. The presence of sub-surface hydrogen atoms was also observed, which indicates the hydride formation that act as an intermediate species for the progression of HER.

3. Results and discussion

The mechanism proposed herein is composed of competing reactions that simultaneously occur at the interface between the Mg surface and the aqueous electrolyte. In this model, anomalous HE proceeds via the reaction of an Mg*H intermediate (the origins of which will be addressed below), which represents adsorbed H (*H) on a metallic surface site, Mg*. The intermediate species Mg*H undergo oxidation upon anodic polarisation, resulting in hydrogen evolution and Mg dissolution (Eq. (1)). This anodic “Heyrovsky-like” reaction is consistent with previous simulations by Surendralal et al. [29], where HE was found to be favoured via an adsorbed H atom on Mg even under anodic polarisation. Furthermore, Adhikari and Hebert [30] showed that dissolution of aluminum in alkaline solutions is mediated by the formation and oxidation of interfacial aluminum hydride. Recently, Binns et al. [31] provided strong evidence for the presence of MgH_2 in the leading edges of a corroding Mg alloy and proposed that anomalous HE on dissolving Mg may be due to chemical decomposition of this MgH_2 species. Even though the hypothesis in this kinetic model that anomalous HE proceeds via the reaction of an Mg*H intermediate is in line with the work by Binns et al. [31], a number of significant differences exist. Briefly, while the formation of a chemical compound (namely MgH_2) is considered by Binns et al. [31], herein a hydrogenated reaction intermediate is assumed. More importantly, the present kinetic model is purely electrochemical with anomalous HE being controlled by the amount of anodic polarisation (Eq. (1)), whereas Binns et al. consider that this phenomenon occurs as a consequence of a chemical reaction independent of potential. Finally, herein a complete reaction mechanism is proposed.

Note that the Mg* created as a result of this reaction allows the surface to continue to react. Even though Eq. (1) is unconventional in the manner it is expressed, with species being simultaneously oxidised (Mg) and reduced (H) in a net anodic process, this representation was

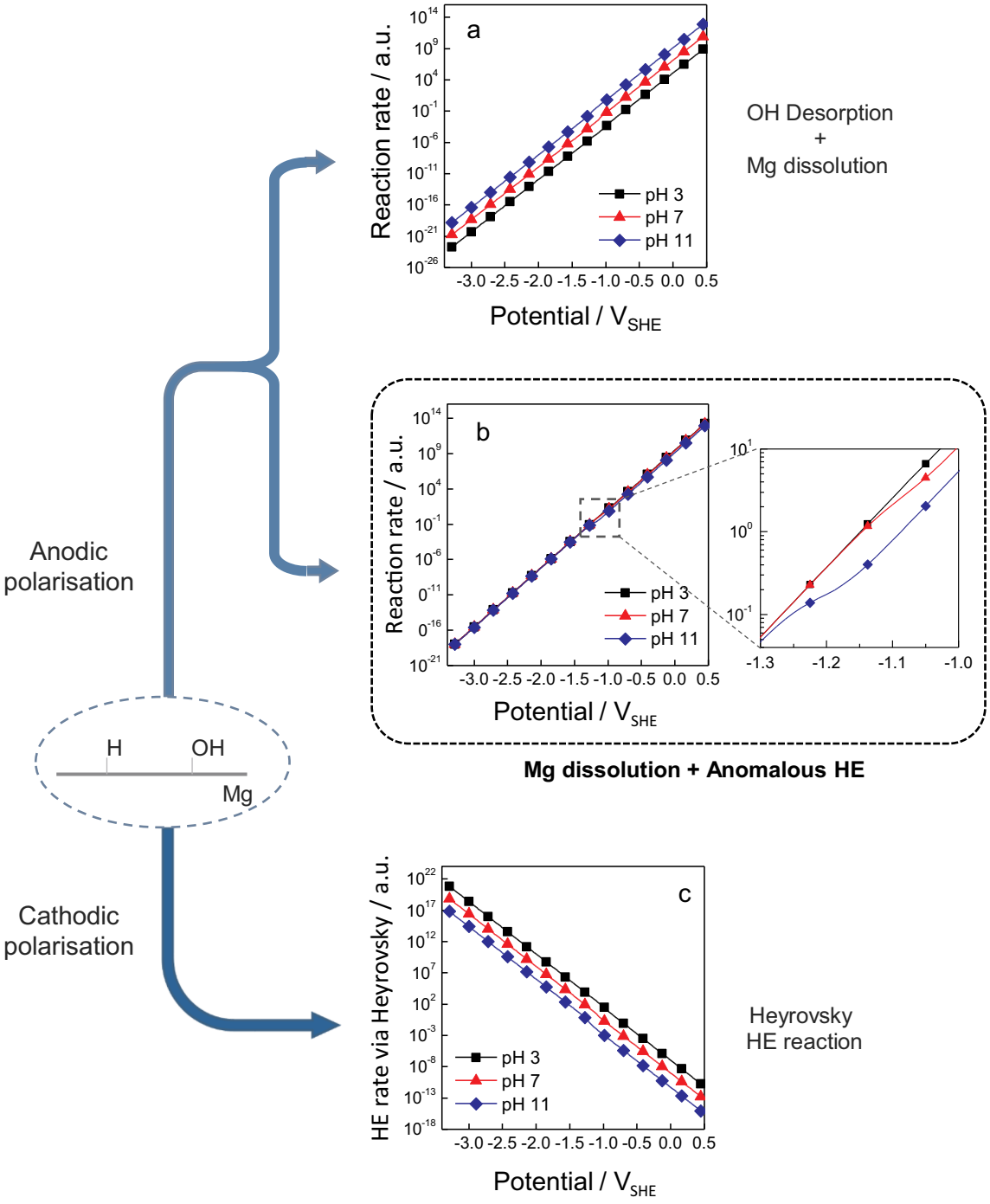

Fig. 3. Kinetic profile at different pH values of various reactions on the Mg(0001) surface plotted as a function of potential.

sought to capture experimental observations whereby Mg dissolution and anomalous HE simultaneously occur on the same Mg active site during anodic polarisation (as shown in Fig. 1). Furthermore, the formulation of the above reaction introduces an original approach to describe an electrochemical process. It comprises an oxidation and a reduction reaction in a global process not as separate half-reactions, but as a net anodic reaction, as depicted by the presence of electrons on the right hand side.

The HER under cathodic polarisation is also proposed to proceed via the Mg*H intermediate. Yuwono et al. [25] demonstrated that, for cathodically polarised Mg, the contribution of the Tafel pathway to the total rate HE is minimal. For this reason, the HER in this model (Eq. (2)) is considered to occur exclusively through the Heyrovsky pathway.

Now that the reaction involved in the origins of the anomalous HE have been introduced, it is necessary to consider the electrochemical reactions involved in creating the Mg*H intermediates. Water-dissociation is a heterolytic reaction that comprises electrochemical half-reactions and co-adsorption of H^+ and OH^- (Eqs. (3) and (4)), and water-assisted Mg dissolution is modelled based on the assumption that it is accompanied by the co-adsorption of H^+ and OH^- (Eqs. (5) and (6)).

Eq. (3) describes the situation for cathodic polarisation during which the Mg*H intermediate will be the only reaction product. However, upon anodic polarisation (Eq. (4)), the formation of the intermediate species Mg*OH is predicted. It is evident from Eq. (4) that, under anodic polarisation, the production of Mg*H will not be

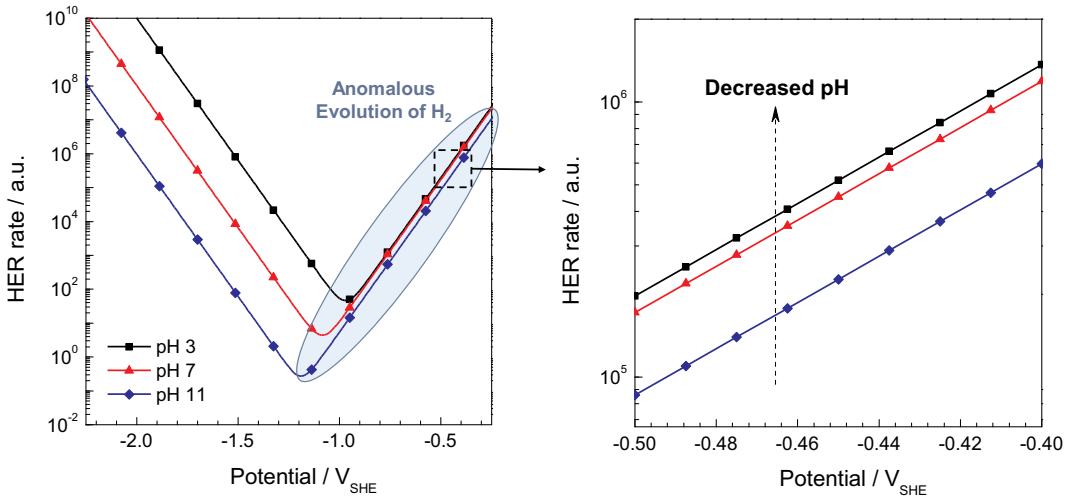

Fig. 4. Kinetic profile of the hydrogen evolution reaction (HER) at different pH values on the Mg(0001) surface plotted as a function of potential.

favoured. Note that this intermediate species is essential for anomalous HE as described by Eq. (1) to proceed. For this reason, we propose that the adsorption of H^+ on the surface to form Mg*H may also occur via Eq. (5), which is a net anodic reaction, with the simultaneous dissolution of Mg.

Assuming that the Mg*H intermediate is a precursor species to H_2 formation during Mg dissolution, Eq. (1) is in accord with vast experimental observations, whereby increased anodic polarisation from the corrosion potential is accompanied by greater rates of HE. Moreover, such reactions (Eqs. (5) and (6)) are also used to quantify the occurrence of water-assisted Mg dissolution. Consequently, the global water-dissociation reaction (Eq. (7)) will be described by a combination of Eqs. (3)–(6).

As depicted by Eq. (7), four available metal sites on the Mg surface (Mg*) are consumed with the subsequent Mg dissolution and the formation of the two intermediate species: Mg*OH and Mg*H.

Finally, it is proposed that, upon anodic polarisation, Mg*OH may undergo desorption from the surface, accompanied by Mg dissolution and the creation of a fresh newly available Mg site for water-dissociation. Together with the Mg dissolution reactions presented in Eqs. (5) and (6), this complementary reaction, OH-assisted Mg dissolution in Eq. (8) is introduced with the aim of preventing the eventual reactive Mg surface blockage by saturation with the Mg*OH intermediate, which would poison both Mg dissolution and the anomalous HE reactions.

The rate associated with the water dissociation reaction (as shown in Fig. 2) indicates that, under cathodic polarisation, the production of Mg*H occurs more rapidly with decreasing potential. The increased concentration of Mg*H intermediates during cathodic polarisation facilitates the HER by the Heyrovsky pathway (Eq. (2)). These assertions are in excellent agreement with experimental observations, where more negative applied potentials are accompanied by increasing rates of HE. However, in the anodic region (potentials above the corrosion potential, as shown in Fig. 2), dissolution of Mg metal may occur with the simultaneous production of Mg*OH and Mg*H, the latter being subsequently involved in the anomalous evolution of H_2 (via Eq. (1)). Compared to previous reports where water dissociation reaction rates increased with polarisation only in a narrow window of potentials, here it is revealed that greater concentrations of Mg*H on the surface are invariably favoured with increasing anodic polarisation.

Once water molecules have been adsorbed on the Mg surface as Mg*H and Mg*OH intermediates, it is necessary to assess the rates at which they will either react to produce H_2 or desorb from the surface to leave fresh available Mg sites for the reaction to continue. Desorption rates of Mg*OH (Eq. (8)) and Mg*H (Eq. (1)) are presented in Fig. 3a and b, respectively. It can be observed that desorption of both intermediate species is favoured with increasing polarisation over the whole range of potentials tested. As expected, under anodic polarisation, desorption of Mg*H and Mg*OH is accompanied with dissolution of Mg metal. Most importantly, simulation results indicate that at increasing positive potentials, fresh available Mg sites are created to further support the water dissociation reaction, preventing the reactive Mg surface blockage by saturation with these adsorbates.

Under cathodic polarisation, the HER proceeds primarily via the Heyrovsky pathway (Eq. (2), as shown in Fig. 3c), with increasing rates of H_2 production as the potential takes more negative values. Note that the cathodic kinetics are pH-dependent, with enhanced rates of HE at a given cathodic potential as the environment near the electrode surface becomes more acidic. This is direct consequence of the water dissociation kinetics, which promote faster adsorption of Mg*H at lower pH values thus favouring the Heyrovsky reaction (see Eq. (2)).

The combined kinetics of all the proposed reactions that lead to HE (both under anodic and cathodic polarisation) indicate that the rate of the HER will increase at potentials below and above E_{corr} (approximately between -1 and -1.2 V_{SHE}) as shown in Fig. 4, which is precisely what has been observed experimentally for a myriad of Mg polarisation studies.

4. Conclusions

The phenomenon of anomalous HE manifests under anodic polarisation; this is at potentials more positive than the corrosion potential, E_{corr}. Calculations presented herein, coupled with a universal reaction scheme, indicate that the Heyrovsky pathway will not contribute to the increased rates of HE. However, it is revealed that HE rates increase with simultaneous dissolution of Mg with increasing potentials. Furthermore, the governing reactions are pH-dependent and reveal higher kinetics at lower pH values. The mechanism of Mg dissolution accompanied with HER at the same active sites is the major contribution of this study – providing a holistic understanding of aqueous corrosion for a widely used metal. Previous ab initio models were unable to explain the increase in HE at anodic potentials due to the saturation of hydrogen on the surface, which created a physical barrier separating Mg active sites and reactive molecules in the electrolyte.

Acknowledgements

SF acknowledges the Spanish State Research Agency (Ministry of Science, Technology and Universities of Spain), the Spanish National Research Council (CSIC) and the European Regional Development Fund (ERDF) for the financial support under the Project MAT2015-74420-JIN

(AEI/FEDER/UE). JAY acknowledges the National Computational Infrastructure (NCI) Raijin and the Pawsey Supercomputing Centre Magnus.

Author contributions

SF and JAY proposed the mechanism and developed the theory. JAY developed the electrochemical kinetic model and performed ab initio calculations. CDT performed ab initio molecular dynamic calculation. CDT, NB and GSF advised on theory and electrochemical kinetic model. All authors participated in writing the paper.

Appendix A. Supplementary data

Supplementary data to this article can be found online at https://doi.org/10.1016/j.elecom.2019.106482.

References

[1] J.O. Bockris, A.K.N. Reddy, Modern Electrochemistry, Kluwer Academic/Plenum Publishing, New York, 2000.
[2] M. Esmaily, J.E. Svensson, S. Fajardo, N. Birbilis, G.S. Frankel, S. Virtanen, R. Arrabal, S. Thomas, L.G. Johansson, Prog. Mater. Sci. 89 (2017) 92–193.
[3] W. Beetz, Philos. Mag. 32 (1866) 269–278.
[4] S. Fajardo, G.S. Frankel, Electrochim. Acta 165 (2015) 255–267.
[5] S. Fajardo, C.F. Glover, G. Williams, G.S. Frankel, Electrochim. Acta 212 (2016) 510–521.
[6] S. Fajardo, C.F. Glover, G. Williams, G.S. Frankel, Corrosion 73 (2017) 482–493.
[7] S. Fajardo, O. Gharbi, N. Birbilis, G.S. Frankel, J. Electrochem. Soc. 165 (2018) C916–C925.
[8] M. Curioni, J.M. Torrescano-Alvarez, Y.F. Yang, F. Scenini, Corrosion 73 (2017) 463–470.
[9] G. Williams, N. Birbilis, H.N. McMurray, Electrochem. Commun. 36 (2013) 1–5.
[10] M. Curioni, Electrochim. Acta 120 (2014) 284–292.
[11] S.H. Salleh, S. Thomas, J.A. Yuwono, K. Venkatesan, N. Birbilis, Electrochim. Acta 161 (2015) 144–152.
[12] N. Birbilis, A.D. King, S. Thomas, G.S. Frankel, J.R. Scully, Electrochim. Acta 132 (2014) 277–283.
[13] M. Curioni, F. Scenini, T. Monetta, F. Bellucci, Electrochim. Acta 166 (2015) 372–384.
[14] T.W. Cain, I. Gonzalez-Afanador, N. Birbilis, J.R. Scully, J. Electrochem. Soc. 164 (2017) C300–C311.
[15] M. Taheri, J.R. Kish, N. Birbilis, M. Danaie, E.A. McNally, J.R. McDermid, Electrochim. Acta 116 (2014) 396–403.
[16] D. Lysne, S. Thomas, M.F. Hurley, N. Birbilis, J. Electrochem. Soc. 162 (2015) C396–C402.
[17] S. Thomas, O. Gharbi, S.H. Salleh, P. Volovitch, K. Ogle, N. Birbilis, Electrochim. Acta 210 (2016) 271–284.
[18] N. Birbilis, T. Cain, J.S. Laird, X. Xia, J.R. Scully, A.E. Hughes, ECS Electrochem. Lett. 4 (2015) C34–C37.
[19] T. Cain, S.B. Madden, N. Birbilis, J.R. Scully, J. Electrochem. Soc. 162 (2015) C228–C237.
[20] D. Mercier, J. Światowska, S. Zanna, A. Seyeux, P. Marcus, J. Electrochem. Soc. 165 (2018) C42–C49.
[21] S.V. Lamaka, D. Höche, R.P. Petrauskas, C. Blawert, M.L. Zheludkevich, Electrochem. Commun. 62 (2016) 5–8.
[22] D. Höche, C. Blawert, S.V. Lamaka, N. Scharnagl, C. Mendis, M.L. Zheludkevich, Phys. Chem. Chem. Phys. 18 (2016) 1279–1291.
[23] E. Michailidou, H.N. McMurray, G. Williams, J. Electrochem. Soc. 165 (2018) C195–C205.
[24] K.S. Williams, J.P. Labukas, V. Rodriguez-Santiago, J.W. Andzelm, Corrosion 71 (2015) 209–223.
[25] J.A. Yuwono, N. Birbilis, C.D. Taylor, K.S. Williams, A.J. Samin, N.V. Medhekar, Corros. Sci. 147 (2019) 53–68.
[26] J.A. Yuwono, N. Birbilis, K.S. Williams, N.V. Medhekar, J. Phys. Chem. C 120 (2016) 26922–26933.
[27] C.D. Taylor, J. Electrochem. Soc. 163 (2016) C602–C608.
[28] G.S. Frankel, S. Fajardo, B.M. Lynch, Faraday Discuss. 180 (2015) 11–33.
[29] S. Surendralal, M. Todorova, M.W. Finnis, J. Neugebauer, Phys. Rev. Lett. 120 (2018) 246801.
[30] S. Adhikari, K.R. Hebert, J. Electrochem. Soc. 155 (2008) C189–C195.
[31] W.J. Binns, F. Zargarzadah, V. Dehnavi, J. Chen, J.J. Noël, D.W. Shoesmith, Corrosion 75 (2019) 58–68.